第 25 卷第 12 期 半 导 体 学 报 Vol. 25, No. 12
2004 年 12 月 CHINESE JOURNAL OF SEMICONDUCTORS Dec., 2004

Fabrication and Characterization of Tunneling Current of Anodic Bonded Dry-Etched MEMS Tunneling Accelerometer

Dong Haifeng, Hao Yilong, Jia Yubin, Yan Guizhen, Wang Ying and Li Ting

(National Key Laboratory of Nano/Micro Fabrication Technology, Institute of Microelectronics, Peking University, Beijing 100871, China)

Abstract: A tunneling accelerometer is fabricated and characterized based on the extension of the silicon-glass anodic-bonding and deep etching releasing process provided by Peking University. The tunneling current under open loop operation is tested in the air by HP4145B semiconductor analyzer, which verifies the presence of tunneling current and the exponential relationship between tunneling gap and tunneling current. The tunneling barrier is extrapolated to be from 1.182 to 2.177eV. The threshold voltages are tested to be 14~16V for most of the devices. The threshold voltages under −1, 0, and +1g are tested, respectively, which shows the sensitivity of the accelerometer is about 87mV/g.

Key words: tunneling effect; accelerometer; MEMS
EEACC: 0580; 7280; 2575
CLC number: TN304 **Document code**: A **Article ID**: 0253-4177(2004)12-1606-06

1 Introduction

Tunneling accelerometer have been researched by many groups[2~10] since the first tunneling accelerometer developed by Quate[1]. Since the tunneling mechanism in a micro tunneling sensor has been described by many authors[2,7~9,11], we will not describe the details here. A novel process is proposed in this paper to fabricate the tunneling accelerometer, which is an extension of the silicon-glass anodic-bonding and deep etching releasing process of Peking University. The process is simple where the single silicon structure avoids the extra investigation of the stress problem caused during the deep boron diffusion process in Refs. [9, 10] and on chip anodic bonding technology instead of epoxy bonding in Refs. [3, 7, 8, 12] makes it easy to volume-produce. ICP technology is firstly used to fabricate a tunneling accelerometer, which can produce much thicker proof mass than the surface technology in Ref. [2]. The process adds a tip generation mask, a tip metalization mask and an extra photoresist ICP mask to the silicon-glass anodic-bonding and deep etching releasing process of Peking University. The relation of tunneling current to the deflect voltage is deduced. We tested the device by HP4145B semiconductor analyzer, which verifies the tunneling current in the sensor. The barrier height and product of spring constant and the nominal distance between the tip and the counter electrode are also extrapolated. Finally, the deflect threshold voltage under −1, 0, and +1g tested, respectively, which shows the close loop

Dong Haifeng male, was born in 1973, PhD candidate. He is engaged in the research on MEMS inertial devices and processes. Email: hfdong@ime.pku.edu.cn
Hao Yilong male, was born in 1963, professor. He is engaged in the research on MEMS.
Received 26 December 2003, revised manuscript received 2 July 2004

sensitivity of the accelerometer is about 87mV/g. The structure parameters are designed by system analysis method[13] and shown in Fig. 1 with the specification object of resolution = 1.023×10^{-6}g/(rt · Hz), threshold voltage = 19.686V and the close loop sensitivity = 93mV/g.

2 Fabrication process

Fabrication of this device is an extension of the silicon-glass anodic-bonding and deep etching releasing process provided by Peking University. It requires one n-type (100) silicon wafers with the height of 400μm and one # 7740 Corning glass wafer. Six masks are used in the process: five for the silicon wafer and one for the glass wafer, as shown in Fig. 2.

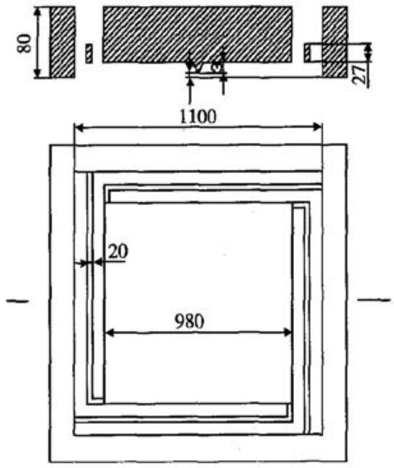

Fig. 1 Schematic of the tunneling accelerometer

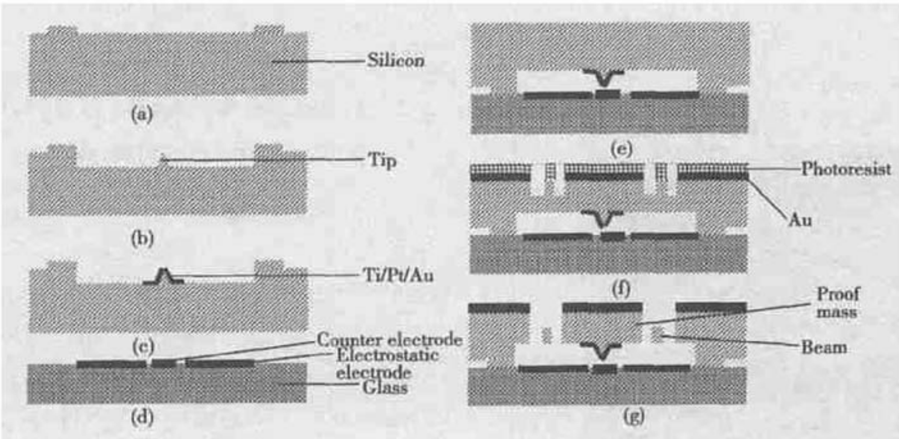

Fig. 2 Fabrication process of the tunneling accelerometer (a) Mask1 KOH etching to define the original gap between the tip and the counter electrode; (b) Mask2 HNA etching to define the tunneling tip; (c) Mask3 Ti30nm/Pt20nm/Au100nm lift-off on the tip; (d) Mask4 Ti30nm/Pt20nm/Au150nm lift-off for the tip counter electrode, electrostatic electrode and lead on the glass; (e) Anodic bonding between the silicon and the glass; (f) Mask5 ICP etching to define the beam; (g) Mask6 ICP etching to release the structure

In the silicon wafer, a 1μm recess is first created by KOH to define the original distance between the tunneling tip and the counter electrode. Next HNA (HNO_3 : HF : CH_3OOH = 30 : 1 : 4) wet etching is performed to fabricate the tip, which is 3μm in height and the top of the tip is a small plane with the area smaller than 0.1μm^2. Then the tip is metallized by sputtering a multilayer of Ti30nm/Pt20nm/Au100nm and lift-off. Figure 3 shows a SEM view of the tunneling tip.

Fig. 3 SEM view of the tunneling tip

Fabrication of the glass substrate wafer starts with creating a recess of 120~ 150nm, then sputtering a multilayer of Ti30nm/Pt20nm/Au150nm and lift-off to generate the metal lead. Before anodic bonding an phosphor diffusion is performed to reduce the resistivity to $R_{\square} < 6\Omega/\square$, anodic bonding is performed to bond the silicon wafer and the glass wafer together, followed by KOH to reduce the thickness of the silicon wafer to about 80μm. Then Al is sputtered and etched to define the proof mass. Next the photoresist is spinned on and exposed to define the width and the length of the supporting beam, followed by ICP process to define the thickness of the supporting beam. The photoresist mask is etched by RIE and another ICP is performed to release the structure. Figure 4 shows a photomicrograph of the completed device and an SEM view of one conner.

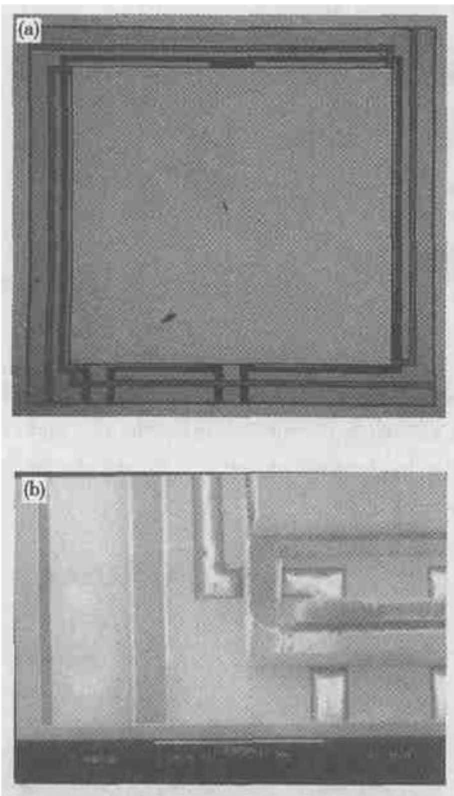

Fig. 4 (a) Photomicrograph of the completed device; (b) SEM view of the bottom left corner of the device

3 Characterization of the tunneling current

3.1 Measurement equipment and its connection with the device

An HP 4145B semiconductor parameter analyzer was employed in the tunneling current characterization of the device in air. There were three channels to be monitored: CH1(V_Q, I_Q) was connected to the bottom deflection electrode which was Ti(30nm)/Pt(20nm)/Au(150nm) in the glass substrate, CH2(V_G, I_G) was connected to the proof-mass and the tunneling tip, CH3(V_T, I_T) was connected to the counter-electrode of the tunneling tip.

3.2 Testing of the current I_T, I_Q before the occurrence of the tunneling current

Firstly V_T is set to 0.05V and V_Q is swept from 0 to 10V to measure the current I_T and I_Q. We find that before the tunneling current occurs there is ultra small current of I_T and I_Q, which is in the order of 10^{-13}~ 10^{-12}A. Figure 5 shows the relation between I_T, I_Q, and V_Q. The inherent resistance of the glass or surface contaminations may cause this current. Because it is very small and its change is in linear relation with the V_Q, its effect on the sensor precision can be neglected.

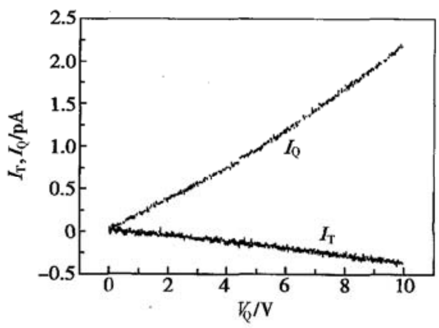

Fig. 5 Relation between I_T, I_Q, and V_Q The equation of the fitted line is also shown in the figure.

3.3 Measurement of the tunneling current versus deflect voltage

The change of the tunneling current I_D versus the deflect voltage V_Q is measured firstly where the tunneling voltage V_T is set to be 0.05V and the proof-mass and the tunneling tip is set to be common (V_G= 0V). While V_Q is swept from 0 to 20V, it is observed that electron tunneling occured at $V_Q \approx 15.9$V (the variation scope is from 14V to 16V for most of the devices), which is smaller than the designed value $V_{Q,th}$ = 19.7V. We explain that is due to the reducing of the initial gap distance between the tip and the counter electrode. The distance before the bonding is measured to be 1.02μm. And the $V_{Q,th}$ show that the distance has been reduced to about 0.66μm.

According to the measured $V_{Q,th}$, we set the sweep voltage of V_Q from 15.5 to 16.5V to investigate the precision change of tunneling current versus deflect electrostatic voltage. We measured four times and the internal of every time is about 2min. Figure 6 shows the curves of the measurement. The threshold voltage (at which the tunneling current occurs) changed from 15.920 to 15.929V, the variation is within 0.06%. It should be pointed out we did not set the restriction of I_T and the value of

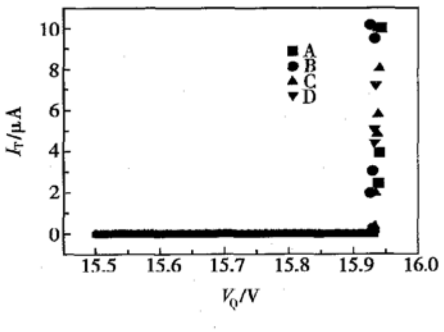

Fig. 6　Four measurement curves of I_T versus V_Q

I_T has been up to 10μA every time, which shows that the tip contacts with the counter electrode. As the variation of the $V_{G,th}$ is only about 0.06%, we can get the conclusion that the contact (not collision) between the tip and the counter electrode has little effect on the $V_{G,th}$.

To verify the tunneling current between the tip and the counter electrode, we deduce the relation between V_Q and I_T and get the following equation

$$\ln I_T \approx \alpha \sqrt{\Phi} k' \times 10^{10} \times V_Q^2 - \alpha \sqrt{\Phi} X_{gap} \times 10^{10} \quad (1)$$

where $k' = \frac{1}{2} \times \frac{\epsilon A}{k X_{tip}^2}$, A is the deflective electrode area, X_{tip} is the tip height, k is the elastic coefficient; α is a constant, Φ is the barrier height.

From Eq. (1), we know that ln I_T and V_Q^2 have a linear relation and the ratio of slope to intercept should be a constant. Figure 7 shows the relation of V_Q^2 to $\ln I_T$ around the threshold voltage. The lin-

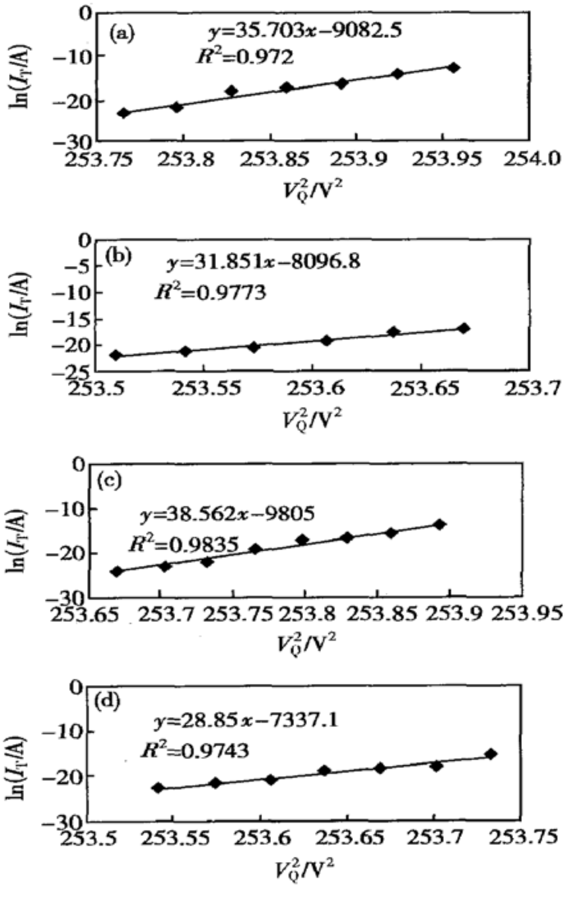

Fig. 7　Curves between the logarithm of the tunneling current and the square of the deflect voltage (a, b, c, d are four measurements respectively)

earized equations are also shown in the figures, from which we can see that the relation of $\ln I_T$ to V_Q^2 fits a straight line very well. The ratio of slope and intercept is calculated to be 254.39, 254.21, 254.26, and 254.31, respectively, and the maxim variation is within 0.07%. The product of spring constant and the original distance between the tip and the electrode can be determined from the ratio to be 1.17×10^{-4}N. The barrier height is extrapolated to be 1.182, 1.499, 1.847, 2.177eV, which are comparable to those reported in Refs. [2, 12].

3.4 Measurement of the threshold V_Q under − 1, 0, and + 1g

After packaging we put one of the devices on the HP4145B box and measure the threshold V_Q under − 1, 0 (turning the box 90°), and 1g (turning the box 180°). Figure 8 shows the curves of I_T versus V_Q and threshold voltage V_Q under − 1, 0, and + 1g, which correspond to the output feedback deflect voltage in a close loop system. The sensitivity of the close loop system is estimated by the offset of the threshold V_Q under − 1, 0, and + 1g to be about 87mV/g which is close to our theoretical design value of 93mV/g.

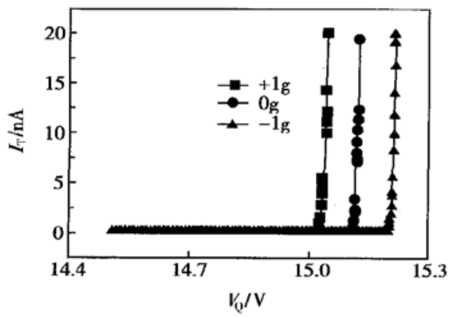

Fig. 8 Curves of I_T versus V_Q that show the changes of threshold voltage V_Q under − 1, 0, and + 1g

4 Noise analysis

There are two kinds of noise for the tunneling devices. One is the noise from the structure, such as the thermal effects, residual stress, etc. Because of the ultra sensitivity of the tunneling devices, some effect that can be ignored in other devices must be considered in the tunneling devices. The other is from the tunneling mechanism itself, such as local rearrangement of the electrode atoms, the absorption-desorption effect[9, 14, 15]. Some researchers think that at low frequencies the noise in the tunneling membrane transducer is dominated by the effects of temperature fluctuations on the transducer structure[14], other researchers show that the noise level in vacuum is about one order of magnitude lower than that in air ambient for Au tip and the $1/f$ noise level increases with increasing tunneling current[15], which mean that the absorption-desorption effect may be the nominated reason of noise. An experiment scheme is designed by our group to investigate this problem, which use the uniform structure and different tip area. Set the tunneling current to the same magnitude and measure the noise, if the noise is in the same order it means that the noise is dominated by the structure, otherwise it means that the noise is dominated by the mechanism itself. The fabrication of the chips is underway.

5 Conclusion

Fabrication and the open loop measurement of a micro accelerometer based on electron tunneling transducers are reported in this paper. The process is an on-chip bonding process. The single silicon beam avoids the warpage of beam caused by deep boron diffusion and the thermal mismatching. Double steps ICP releasing method achieves a thick proof mass and thin beams while no striction and contamination problem needs to be considered. The open loop measurements verify that the sensor is actually tunneling. The threshold voltage, barrier height and product of spring constant and the nominal distance between the tip and the counter electrode are measured and extrapolated, which provide necessary information for the later feedback circuit and controller design. The − 1, 0, and + 1g deflect threshold show that the accelerometer have a close loop sensitivity about 87mV/g.

Acknowledgements The authors would like to thank Professor Ning Baojun for her assistance in the testing and measurements. We also appreciate the help of staffs in the IME of Peking University for their help in the process. We would also like to acknowledge helpful discussions on structure design and fabrication process with Dr Yang Zhengchuan, Dr Ruan Yong and Dr Zhu Yong.

References

[1] Baski A A, Albrecht T R, Quate C F. Tunneling acelerometer. J Microscopy, 1988, 152: 73

[2] Kubena R L, Atkinson G M, Robinson W P, et al. A new miniaturized surface micromachined tunneling accelerometer. IEEE Electron Device Lett, 1996, 17(6): 306

[3] Rockstad H K, Tang T K, Reynolds J K, et al. A minature, high-sensitivity, electron tunneling accelerometer. Sensors and Actuators, 1996, A53: 227

[4] Pusateri M A, Schiano J L, Vatannia S. A force rebalance accelerometer for an atmospheric weather probe. Proceedings of the American Control Conference, 1997: 816

[5] Zavracky P M, McClelland B, Warner K. Design and process considerations for a tunneling tip accelerometer. J Micromech Microeng, 1996: 352

[6] Scheeper P R, Reynold J K, Kenny T W. Development of a modal analysis accelerometer based on a tunneling displacement transducer. International Conference on Solid State Sensors and Actuators, Chicago, 1997: 867

[7] Liu C H, Kenny T W. A high-precision, wide-bandwith micromachined tunneling accelerometr. J Microelectromech Syst, 2001, 10(3): 425

[8] Liu C H, Barzilai A M, Reynolds J K, et al. Characterization of a high-sensitivity micromachined tunneling accelerometer with micro-g resolution. J Microelectromech Syst, 1998, 7(2): 235

[9] Yeh C, Najafi K. A low-voltage tunneling-based silicon microaccelerometer. IEEE Trans Electron Devices, 1997, 44(11): 1875

[10] Yeh C, Najafi K. CMOS interface circuitry for a low-voltage micromachined tunneling accelerometer. J Microelectromech Syst, 1998, 7(1): 6

[11] Wang Jing, Zhao Yongjun, Cui Tianhong, et al. Synthesis of the modeling and control systems of a tunneling accelerometer using the Matlab simulation. J Micromech Microeng, 2002, 12: 730

[12] Kenney T W, Waltman S B, Reynolds J K, et al. Micromachined silicon tunnel sensor for motion detection. Appl Phys Lett, 1991, 58: 100

[13] Dong Haifeng, Jia Yubin, Hao Yilong, et al. System analysis and design of a micromachined tunneling accelerometer. 5th International Symposium on Test and Measurement, 2003: 21

[14] Grade J, Barzilai A, Reynolds J K, et al. Low frequency drift in tunnel sensor. International Conference on Solid-State Sensors and Actuators, 1997: 871

[15] Wang Jianchao, Zavracky P M, McGruer N E, et al. Study of tunneling noise using surface micromachined tunneling tip devices. International Conference on Solid-State Sensors and Actuators, 1997: 467

基于阳极键合干法刻蚀技术的 MEMS 隧道加速度计的加工及测试

董海峰　郝一龙　贾玉斌　闫桂珍　王　颖　李　婷

(北京大学微电子学研究院 微米/纳米加工技术国家重点实验室, 北京　100871)

摘要: 提出了一种基于北京大学硅玻璃键合深刻蚀释放工艺的扩展工艺, 用来加工微型隧道加速度计. 采用 HP4145B 半导体分析仪在大气环境下对所加工的器件进行了开环测试, 验证了隧道电流的存在以及隧道间隙与隧道电流之间的指数关系. 实验结果外推出的隧道势垒的范围为 1.182~ 2.177eV. 大部分器件的开启电压在 14~16V 之间. 在- 1, 0 和+ 1g 三种状态下对开启电压分别进行了测试, 得到加速度计的灵敏度约为 87mV/g.

关键词: 隧道效应; 加速度计; 微机电系统

EEACC: 0580; 7280; 2575

中图分类号: TN304　　**文献标识码:** A　　**文章编号:** 0253-4177(2004)12-1606-06

董海峰　男, 1973 年出生, 博士研究生, 研究方向为 MEMS 惯性器件与工艺.

郝一龙　男, 1963 年出生, 教授, 博士, 研究方向为微电子机械系统.

2003-12-26 收到, 2004-07-02 定稿